

# Identification of a novel immune infiltration-related gene signature, *MCEMP1*, for coronary artery disease

Wei Ye<sup>1,2,3,4</sup>, Bo Shen<sup>2,3</sup>, Qizhu Tang<sup>2,3</sup>, Chengzhi Fang<sup>1</sup>, Lei Wang<sup>5</sup>, Lili Xie<sup>1</sup> and Qi He<sup>1</sup>

<sup>1</sup> Department of Neonatology, Renmin Hospital of Wuhan University, Wuhan, China

<sup>2</sup> Department of Cardiology, Renmin Hospital of Wuhan University, Wuhan, China

<sup>3</sup> Hubei Key Laboratory of Metabolic and Chronic Diseases, Wuhan, China

<sup>4</sup> Central Laboratory, Renmin Hospital of Wuhan University, Wuhan, China

<sup>5</sup> Department of Cardiology, HanChuan Hospital, Hanchuan, China

## ABSTRACT

**Background:** This study aims to identify a novel gene signature for coronary artery disease (CAD), explore the role of immune cell infiltration in CAD pathogenesis, and assess the cell function of mast cell-expressed membrane protein 1 (*MCEMP1*) in human umbilical vein endothelial cells (HUVECs) treated with oxidized low-density lipoprotein (ox-LDL).

**Methods:** To identify differentially expressed genes (DEGs) of CAD, datasets [GSE24519](#) and [GSE61145](#) were downloaded from the Gene Expression Omnibus (GEO) database using the R “limma” package with  $p < 0.05$  and  $|\log_2 FC| > 1$ . Gene ontology (GO) and pathway analyses were conducted to determine the biological functions of DEGs. Hub genes were identified using support vector machine-recursive feature elimination (SVM-RFE) and least absolute shrinkage and selection operator (LASSO). The expression levels of these hub genes in CAD were validated using the [GSE113079](#) dataset. CIBERSORT program was used to quantify the proportion of immune cell infiltration. Western blot assay and qRT-PCR were used to detect the expression of hub genes in ox-LDL-treated HUVECs to validate the bioinformatics results. Knockdown interference sequences for *MCEMP1* were synthesized, and cell proliferation and apoptosis were examined using a CCK8 kit and Muse<sup>®</sup> Cell Analyzer, respectively. The concentrations of IL-1 $\beta$ , IL-6, and TNF- $\alpha$  were measured with respective enzyme-linked immunosorbent assay (ELISA) kits.

**Results:** A total of 73 DEGs (four down-regulated genes and 69 up-regulated genes) were identified in the metadata ([GSE24519](#) and [GSE61145](#)) cohort. GO and Kyoto Encyclopedia of Genes and Genomes (KEGG) analysis results indicated that these DEGs might be associated with the regulation of platelet aggregation, defense response or response to bacterium, NF-kappa B signaling pathway, and lipid and atherosclerosis. Using SVM-RFE and LASSO, seven hub genes were obtained from the metadata. The upregulated expression of *DIRC2* and *MCEMP1* in CAD was confirmed in the [GSE113079](#) dataset and in ox-LDL-treated HUVECs. The associations between the two hub genes (*DIRC2* and *MCEMP1*) and the 22 types of immune cell infiltrates in CAD were found. *MCEMP1* knockdown accelerated cell proliferation and suppressed cell apoptosis for ox-LDL-treated HUVECs.

Submitted 14 June 2024

Accepted 29 August 2024

Published 25 September 2024

Corresponding authors

Bo Shen, shenbowhdx@126.com

Qizhu Tang, qztang@whu.edu.cn

Academic editor

Fanglin Guan

Additional Information and  
Declarations can be found on  
page 16

DOI [10.7717/peerj.18135](https://doi.org/10.7717/peerj.18135)

© Copyright  
2024 Ye et al.

Distributed under  
Creative Commons CC-BY 4.0

OPEN ACCESS

Additionally, *MCEMP1* knockdown appeared to decrease the expression of inflammatory factors IL-1 $\beta$ , IL-6, and TNF- $\alpha$ .

**Conclusions:** The results of this study indicate that *MCEMP1* may play an important role in CAD pathophysiology.

**Subjects** Cell Biology, Cardiology, Data Mining and Machine Learning

**Keywords** Coronary artery disease, Machine learning algorithm, Immune cell infiltration, *MCEMP1*, ox-LDL treatment HUVECs cells

## INTRODUCTION

Coronary artery disease (CAD) is characterized by the accumulation of atherosclerotic plaque, formed by lipid and immune cells, in the coronary arteries (*Medina-Leyte et al., 2021*). The Global Burden of Disease study estimated that the global prevalence of CAD, at 154 million, accounted for 32.7% of the total global burden of cardiovascular disease in 2016 (*GBD 2016 Disease and Injury Incidence and Prevalence Collaborators, 2017*).

According to China's cardiovascular diseases report in 2018, there were approximately 290 million patients with cardiovascular disease in the country (*Ma et al., 2020*).

Epidemiological studies have shown that older age, male sex, hypertension, diabetes, obesity, hyperlipidemia, smoking, and a sedentary lifestyle all increase the risk of CAD (*Malakar et al., 2019*). CAD is a complex disease influenced by the interactions between genetic and environmental factors. Previous studies have identified several CAD-related genes, such as *CKDN2A*, *CDNK2B*, *GUCY1A3*, and *NOS3* (*Ehret et al., 2016; Harismendy et al., 2011*). Additionally, several CAD risk-related gene expression patterns have been identified using RNAseq technique (*Wang et al., 2021; Kalayinia et al., 2018*). Microarray analysis is a widely used research method for screening novel biomarkers for diagnosis, predicting disease severity, and identifying new drug targets (*Behzadi & Ranjbar, 2019*). For instance, one study found that *BTRC*, *FBXL4*, and *ASB1* genes were downregulated in CAD, while *UBE2D2* was upregulated (*Chen et al., 2021*).

The Gene Expression Omnibus (GEO) database is a publicly available website supported by National Center for Biotechnology information (NCBI), which is utilized for identifying key genes and underlying mechanisms in disease onset and progression (*Barrett et al., 2013*). With the continuous development and widespread application of bioinformatics, many algorithms, such as those based on machine learning algorithms, have been widely applied in cancer research (*Zhao et al., 2022; Donovan et al., 2018; Li et al., 2020*). Studies have also demonstrated that machine-learning algorithms are highly effective for risk prediction and for screening potential CAD biomarkers (*Balashanmugam et al., 2019; Qi et al., 2020*).

Many inflammatory biomarkers, primarily cytokines, acute phase proteins, and cell surface receptors of dividing cells, have been identified as being associated with CAD in some way (*Kott et al., 2020*). The extent of inflammatory cell infiltration into the adventitia has also been found to be related to the severity of atherosclerotic plaques (*Milutinović, Šuput & Zorc-Pleskovič, 2020*). Furthermore, immune checkpoint suppression therapy has been associated with an increased proportion of inflammatory CD3 T cells and CD68

macrophages in coronary atherosclerotic plaques (Newman & Stone, 2019). These cumulative findings indicate that immune cell infiltration plays a crucial role in the development and progression of CAD.

In this study, a differentially expressed gene (DEG) analysis was conducted between healthy samples and CAD samples from the GEO database. Potential hub genes for CAD were identified using machine learning algorithms. Additionally, the relationship between immune cell infiltration and the identified hub genes of CAD was characterized. The expression levels of these hub genes were validated in oxidized low-density lipoprotein (ox-LDL) treatment human umbilical vein endothelial cells (HUVECs), and the cell function of *MCEMP1* in ox-LDL-treated HUVECs was also investigated.

## METHODS

### Screening and enrichment analysis of differentially expressed genes (DEGs)

The GEO DataSets database stores curated gene expression DataSets, as well as original Series and Platform records in the GEO repository (<https://www.ncbi.nlm.nih.gov/gds/?term=>). CAD-related gene expression data (GSE24519, GSE61145, and GSE113079) was obtained from the GEO DataSets database. The GSE24519 and GSE61145 datasets, used as the metadata datasets, included 67 CAD patient samples and 21 normal control samples, and the GSE113079 dataset, used as a validation dataset, included 93 CAD patient samples and 48 normal control samples. All samples from these databases were derived from human peripheral blood.

The R “SVA” package (<https://rdrr.io/bioc/sva/src/R/sva-package.R>) was used for background correction and standardization of the metadata. DEGs between CAD samples and normal samples were identified using the R “limma” package (<https://bioconductor.org/packages/release/bioc/html/limma.html>) with a significance threshold of  $p < 0.05$  and  $|\log_2 FC| > 1$ . Volcano and heat maps were generated using the online SangerBox software (<http://sangerbox.com/>). Gene ontology (GO) and pathway analyses were conducted to identify the biological functions of DEGs, performed using the R “clusterProfiler” package (<https://guangchuangyu.github.io/software/clusterProfiler/>) and Metascape database (<http://metascape.org>).

### Selection and verification of hub genes

Two machine learning algorithms—support vector machine-recursive feature elimination (SVM-RFE) and least absolute shrinkage and selection operator (LASSO)—were applied to search for CAD-related gene signatures in the metadata cohort. The SVM-RFE algorithm (<https://github.com/johncolby/SVM-RFE>) was implemented using the R “mlbench” and “caret” packages, while the LASSO model (<https://glmnet.stanford.edu/>) was executed by the R “glmnet,” “survival,” and “survminer” packages. A Venn diagram was plotted using the R “VennDiagram” package to display the intersection of hub genes filtered by both the SVM-RFE and LASSO algorithms.

The GSE113079 dataset was employed to validate the expression of overlapping gene signatures between CAD patients and the control group.

## Association between CAD-related candidate gene signatures and immune-related features

The CIBERSORT program (<https://cibersortx.stanford.edu/>) was utilized to quantify the proportion of immune cell infiltration (22 different cell types) in CAD gene expression profiles using the R “ggplot2,” “corrplot,” and “forcats” packages. A gene set enrichment analysis (GSEA, <https://www.broadinstitute.org/gsea/>) was conducted to explore the underlying functional mechanisms of the hub genes using the R “ggplot2,” “clusterProfiler,” “enrichplot,” and “ggridges” packages.

## HUVEC culture and treatment

Human umbilical vein endothelial cells (HUVECs) were purchased from iCell Bioscience (iCell-h110; iCell Bioscience, Shanghai, China). These HUVECs were cultured within an endothelial cell growth medium (PriMed-iCell-002, Shanghai, China) supplemented with 5% (v/v) FBS, 1% endothelial cell growth supplement (ECGS), and 1% penicillin streptomycin at 37 °C in 5% CO<sub>2</sub>. HUVECs within passages 3–7 were applied for the experiments. Then, human ox-LDL (Yiyuan Biotechnologies, Guangzhou, China) at concentrations of 50 and 100 µg/mL were added into the cell cultures according to the experimental requirements (*Kang et al., 2021; Di et al., 2021*).

Knockdown interference sequences for *MCEMP1* were provided by GenePharma (Shanghai, China). The optimal working concentration of these interference sequences was selected experimentally prior to the formal experiments. The interference sequence information for *MCEMP1* is as follows: si*MCEMP1*#1, sense 5'-GACCCAGACUAUGA GAAUATT-3', anti-sense 5'- UAUUCUCAUAGUCUGGGUCTT-3', si*MCEMP1*#2, sense 5'-CAGCCUUCAUCAUGGUGAATT-3', anti-sense 5'-UUCACCAUGAUGAA GGCUGTT-3', si*MCEMP1*#3, sense 5'-GAGCAAGAUUGAUAGAUAUATT-3', anti-sense 5'-UAAUCUAUCAAAUCUUGCUCTT'.

## Cell proliferation and apoptosis assay

After a 24-h treatment with ox-LDL,  $2 \times 10^3$  cells (100 µL) were inoculated within each well of the 96-well culture plate. About 3–4 h later, when cells had adhered to the wall, 100 µL of RPMI 1,640 complete medium and 10 µL of CCK-8 were added. Then, the cells were cultured in 5% CO<sub>2</sub> at 37 °C for 2 h. The OD450 values were determined with a microplate reader (Infinite M200, Tecan, Salzburg, Austria) at the wavelength of 450 nm.

The Muse<sup>®</sup> Cell Analyzer (Milipore, Burlington, MA, USA) was used to assess the effects of *MCEMP1* on apoptosis in ox-LDL treated HUVECs. The cells were suspended in 100 µL of 1% BSA, and an equal volume of apoptosis working fluid was added. Apoptosis was detected after 20 min of gentle resistance. HUVECs were harvested after the indicated treatments, re-suspended at a concentration of  $10^6$ /mL, and stained with a Muse Annexin V & Dead Cell Kit in darkness. The Muse<sup>®</sup> Cell analyzer (CogtoFLEX, BECKMAN) was used to quantify the percentage of apoptotic cells. The apoptotic rate was defined as the percentage of “UR+LR” cells.

### Lactate dehydrogenase (LDH) and nitric oxide (NO) assay

HUVECs were cultured in 96-well plates at a density of  $1 \times 10^4$  cells/mL, and pretreated with ox-LDL (100  $\mu\text{g}/\text{mL}$ ) for 48 h. The supernatants from ox-LDL treated HUVEC were collected by centrifugation at 5,000  $g$  for 10 min. Then, the LDH content and NO content in the media was assessed using an LDH activity kit (BC0685; Solarbio, Beijing, China) and a NO assay kit (AKNM005C; Boxbio, Beijing, China), respectively.

### Quantitative real-time polymerase chain reaction (qRT-PCR)

Total RNA was extracted from the HUVECs using TRIzol reagent (Accurate Biology, Changsha, China). The RNA was reverse-transcribed into cDNA using a PrimeScript RT Reagent Kit (TakaRa Biotechnology, Dalian, China). Real-time PCR was performed using SYBR green fluorescence (TakaRa) for the relative quantification of mRNA expression. Quantification was achieved using the  $2^{-\Delta\Delta C_t}$  method, with GAPDH used to normalize mRNA levels. The following primers were used in this study: *DIRC2* forward primer: 5'-GTCCATAGTTGGAGGCTGTGTTG-3' and reverse primer: 5'-ACGTGGATGACAGTGCTAGCTCC-3'; *MCEMP1* forward primer: 5'-CTGAGATGTCCAAGGAGCTGCT-3' and reverse primer: 5'-TGGTGATGCTCTGCTGAACGGA-3'; GAPDH forward primer: 5'-GGAGCGAGATCCCTCCAAAAT-3' and reverse primer: 5'-GGCTGTTGTCATACTTCTCATGG-3'.

### Western blotting

Proteins were extracted from HUVECs using RIPA lysis buffer (Solarbio, Beijing, China) for 20 min, followed by centrifugation at 12,000 rpm for 15 min at 4 °C to collect the proteins. Protein concentrations were measured by a BCA protein assay kit (Beyotime, Shanghai, China). Equal amounts of proteins (60  $\mu\text{g}$ ) and a pre-stained protein ladder (YESEN, Shanghai, China) were separated by 10% SDS-PAGE gel, electro-transferred to nitrocellulose membranes, and incubated with primary antibodies overnight at 4 °C. The anti-*DIRC2* antibody (1:1,000, 26750-1-AP; Proteintech), anti-*MCEMP1* antibody (1:3,000, 25700-1-AP, proteintech), anti-ICAM1 antibody (1:500, 200350-F12; ZEN BIO), and anti-GAPDH antibody (1:2,000, 60004-1-Ig; Proteintech) were used in this study. The membranes were incubated with secondary antibodies for 1.5 h at room temperature. Bands with antigen-antibody complexes were visualized using Immobilon ECL substrate (YESEN, Shanghai, China), and the blots were imaged with an E-BLOT luminescent image analyzer (e-BLOT, Shanghai, China).

### Enzyme-linked immunosorbent assay (ELISA)

HUVECs were cultured in 96-well plates at a density of  $1 \times 10^4$  cells/mL and pretreated with ox-LDL (100  $\mu\text{g}/\text{mL}$ ) for 48 h. The cultured HUVEC supernatants were collected by centrifugation at 5,000  $g$  for 10 min. The levels of IL-1 $\beta$ , IL-6, and TNF- $\alpha$  were detected using respective ELISA kits (Jianglai Biotechnology, Shanghai, China).

## RESULTS

### Screening and enrichment analyses of DEGs in CAD

In our study, a comprehensive analysis was conducted to identify DEGs in CAD. A total of 73 DEGs (four down-regulated genes and 69 up-regulated genes, [Table S1](#)) were discovered between 67 CAD patient samples and 21 normal control samples from the metadata cohorts ([GSE24519](#) and [GSE61145](#)) cohort. Volcano ([Fig. 1A](#)) and heatmap ([Fig. 1B](#)) plots depicted these DEGs.

Further functional characterization of these DEGs was performed using GO and Kyoto Encyclopedia of Genes and Genomes (KEGG) pathway analyses. The GO analysis ([Fig. 1C](#)) results indicated potential associations of DEGs with a range of biological processes, including the regulation of platelet aggregation, defense response or response to bacterium, regulation of aspartic-type endopeptidase activity involved in the amyloid precursor protein catabolic process, regulation of homotypic cell-cell adhesion, and positive regulation of cytokine production. Additionally, the KEGG pathway analysis ([Fig. 1D](#)) revealed significant involvement of DEGs in pathways such as the NF-kappa B signaling pathway, lipid and atherosclerosis, the B cell receptor signaling pathway, the IL-17 signaling pathway, among others.

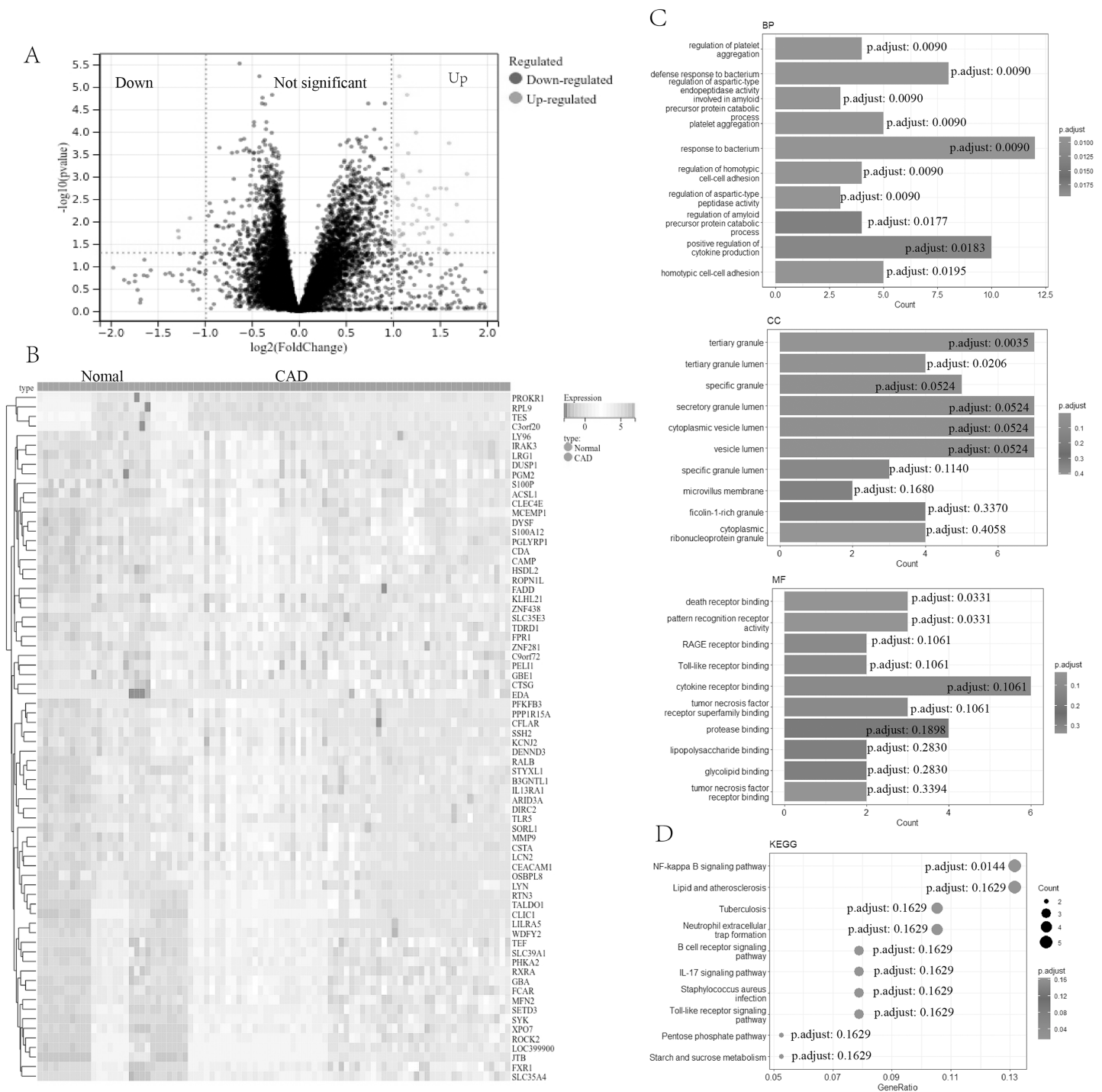
### Selection and verification of hub genes

To identify key genes that might serve as potential biomarkers or therapeutic targets, SVM-RFE and LASSO logistic regression algorithms were employed. The SVM-RFE algorithm identified 18 gene signatures in the determined DEGs ([Fig. 2A](#)), while the LASSO logistic regression algorithm recognized 16 gene signatures ([Fig. 2B](#)). Through intersection analysis, seven overlapping hub genes (*HSDL2*, *PGLYRP1*, *CAMP*, *MCEMP1*, *IRAK3*, *DIRC2*, and *PFKFB3*) were finally selected in the metadata cohort ([Fig. 2C](#)).

The [GSE113079](#) dataset (93 CAD patient samples and 48 normal samples) was used to validate the accuracy of the approach and the expression levels of the seven hub genes ([Fig. 2D](#)). Notably, the expression levels of *PGLYRP1* and *IRAK3* were not detected in the validation set. Furthermore, *CAMP* and *HSDL2* expression levels did not show significant differences between CAD and normal samples. Interestingly, *PFKFB3* expression was found to be down-regulated in CAD samples, contrasting with the metadata results. However, *DIRC2* ( $p = 0.011$ ) and *MCEMP1* ( $p = 0.00047$ ) were significantly up-regulated in CAD samples compared to control samples, aligning with the metadata. Therefore, *DIRC2* and *MCEMP1* were selected for further investigation in the follow-up studies.

### Correlation of DIRC2 and MCEMP1 with immune cell infiltration and signal pathways

In our study, we investigated the correlation between the expression levels of two key genes, *DIRC2* and *MCEMP1*, and the infiltration of immune cells in CAD tissues. The proportions of 22 different types of immune cell infiltrates were calculated and compared between CAD and normal tissue ([Fig. S1A](#)). Our findings revealed that the degree of infiltration of regulatory T cells (Tregs,  $p = 4.3e-4$ ), resting dendritic cells ( $p = 8.4e-4$ ), and



Full-size DOI: [10.7717/peerj.18135/fig-1](https://doi.org/10.7717/peerj.18135/fig-1)

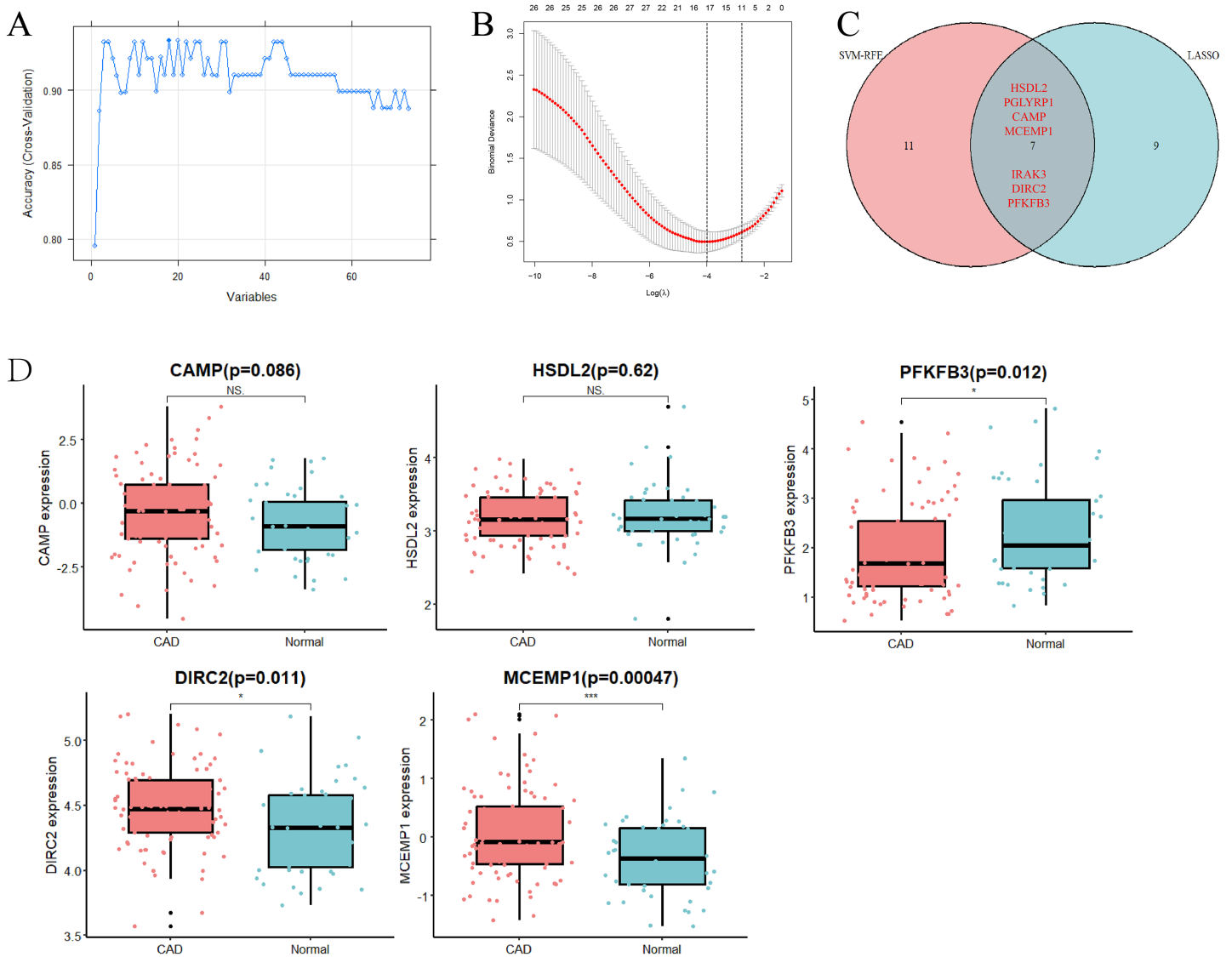


**Figure 2** Selection and verification of diagnostic hub genes. (A) Accuracy of candidate gene selection in the SVM-RFE algorithm. (B) Coefficient profiles of candidate genes in the LASSO model. (C) Venn diagram showing the overlap of characteristic genes of the two algorithms. (D) Bar chart for validation of the expression of candidate diagnostic markers in the GSE113079 dataset. Red represents the case group and blue represents the control group. \* $p < 0.05$ ; \*\*\* $p < 0.001$ ; NS, not significant. SVM-RFE, support vector machine-recursive feature elimination; LASSO, least absolute shrinkage and selection operator. Full-size [DOI: 10.7717/peerj.18135/fig-2](https://doi.org/10.7717/peerj.18135/fig-2)

resting mast cells ( $p = 0.03$ ) in CAD tissues was lower than in normal tissues. Conversely, CAD samples displayed a higher infiltration of activated mast cells ( $p = 6.3e-3$ ) and neutrophils ( $p = 1.2e-3$ ). Additionally, the correlation among these infiltrating immune cells was calculated (Fig. S1B), showing that activated mast cells had a negative correlation with resting mast cells but a positively associated with neutrophils.

The relationships between the two hub genes (*DIRC2* and *MCEMP1*) and the 22 types of immune cell infiltrates in CAD were further explored (Figs. 3A and 3B). *DIRC2* was negatively associated with regulatory T cells (Tregs,  $p < 0.001$ ), CD8 T cells ( $p = 0.001$ ), resting dendritic cells ( $p = 0.015$ ), and CD4 memory activated T cells ( $p = 0.033$ ), but



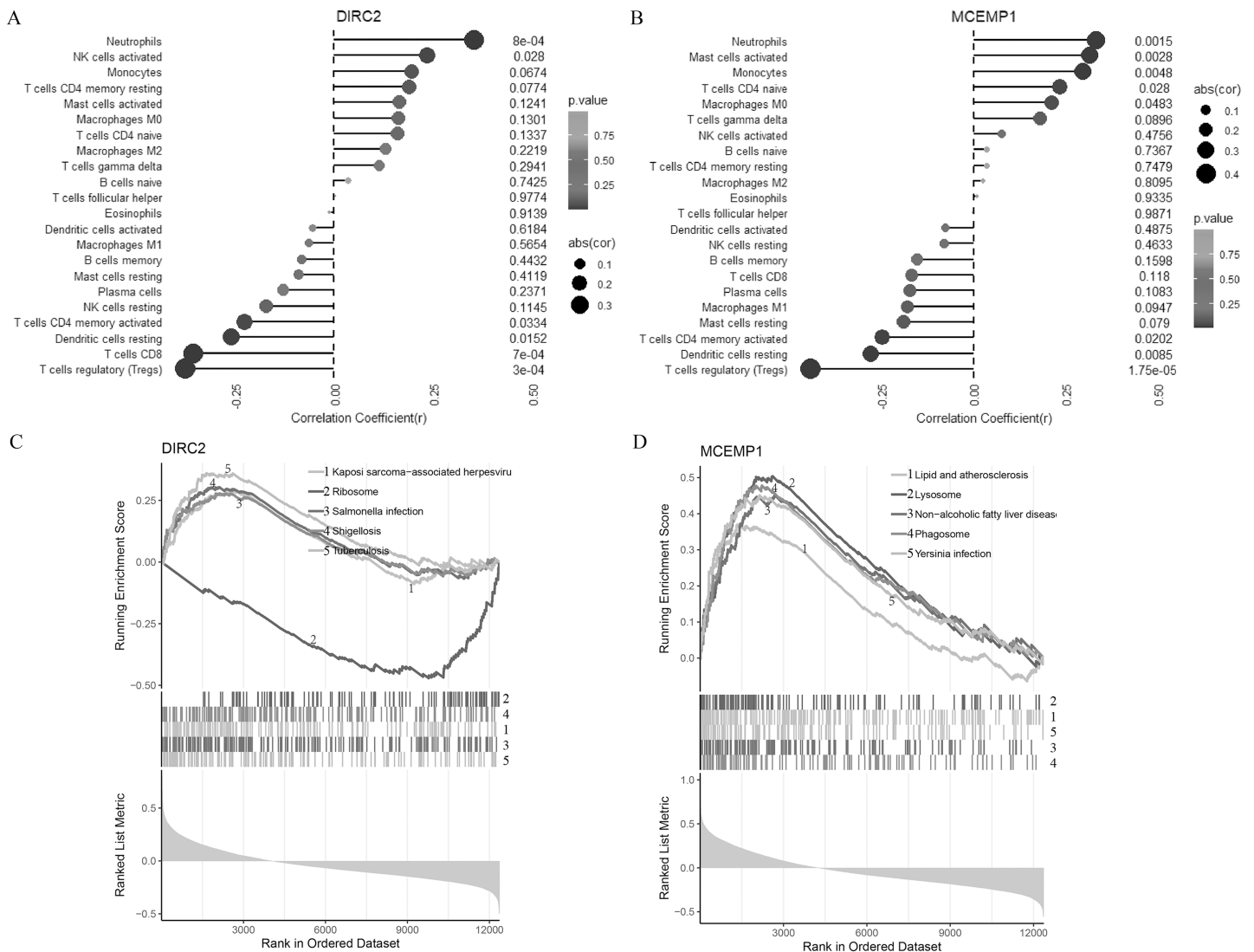


**Figure 3** Correlation of two diagnostic markers with immune cell infiltration and signal pathway. Lollipop chart for immune cell infiltration with *DIRC2* (A) and *MCEMP1* (B). Line graph GSEA analysis for the top five pathways of *DIRC2* (C) and *MCEMP1* (D).

Full-size DOI: 10.7717/peerj.18135/fig-3

positively associated with activated NK cells ( $p = 0.028$ ) and neutrophils ( $p = 0.001$ , Fig. 3A). Similarly, *MCEMP1* was negatively associated with regulatory T cells (Tregs,  $p < 0.001$ ), resting dendritic cells ( $p = 0.009$ ), and CD4 memory activated T cells ( $p = 0.020$ ), but positively associated with macrophages M0 ( $p = 0.048$ ), CD4 naive T cells ( $p = 0.028$ ), monocytes ( $p = 0.005$ ), activated mast cells ( $p = 0.003$ ), and neutrophils ( $p = 0.002$ , Fig. 3B).

To further understand the potential roles of *DIRC2* and *MCEMP1* in the pathogenesis of CAD, GSEA was used to identify the related signal pathways (Figs. 3C and 3D). *DIRC2* was positively linked to Kaposi sarcoma-associated herpesvirus, salmonella infection, shigellosis, and tuberculosis, and negatively linked to ribosomes (Fig. 3C). On the other hand, *MCEMP1* was positively linked to lipid and atherosclerosis, lysosomes,

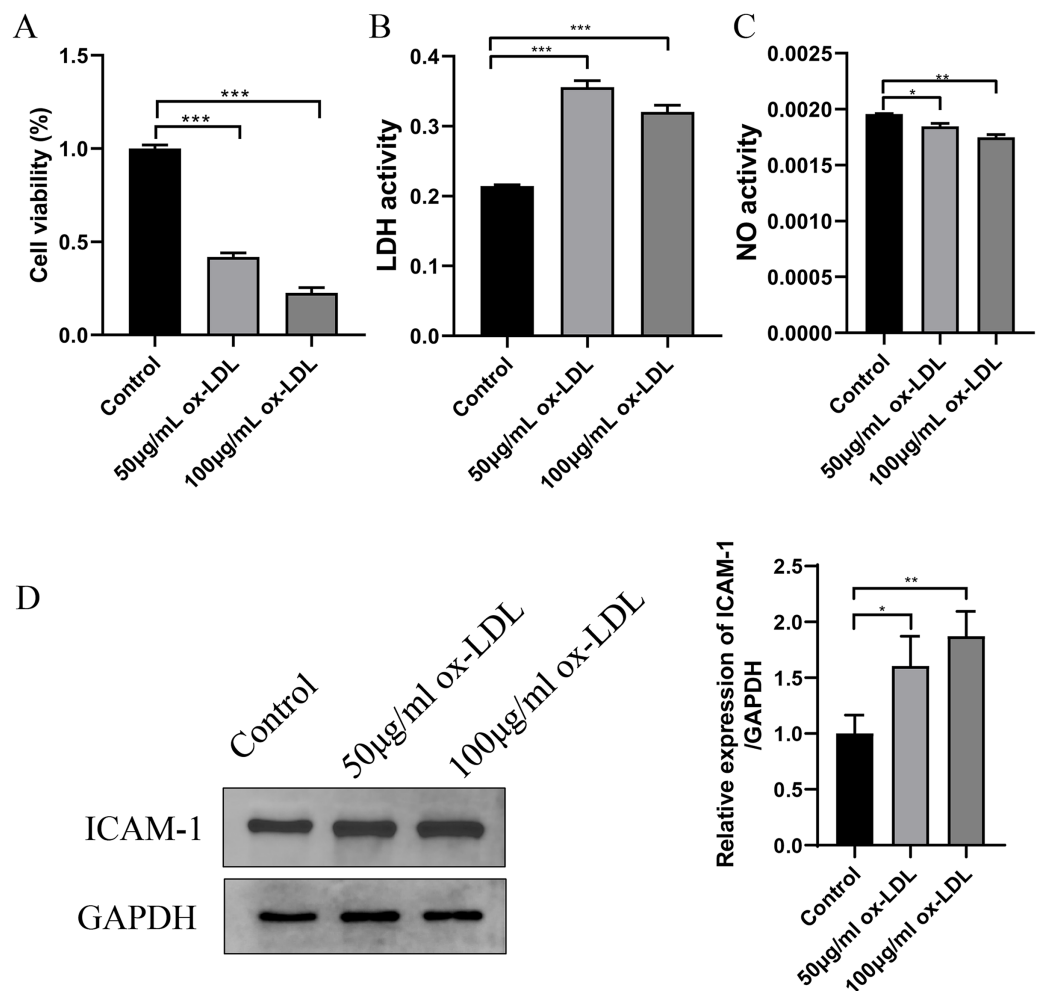


**Figure 4** Establishment of ox-LDL-treated HUVECs. (A) Cellular viability was detected by CCK-8 assay, which was normalized to the control group. (B and C) LDH and NO levels in ox-LDL-treated HUVECs were analyzed by chromometry using commercially available assay kits. (D) The expression of ICAM-1 was detected by western blot assay. \* $p < 0.05$ ; \*\* $p < 0.01$ ; \*\*\* $p < 0.001$ .

Full-size DOI: 10.7717/peerj.18135/fig-4

non-alcoholic fatty liver disease, phagosomes, and *Yersinia* infection (Fig. 3D). These findings indicate that *DIRC2* and *MCEMP1* may play an important role in the pathogenesis of CAD, potentially through their involvement in these immune-related signaling pathways.

### The expression of *DIRC2* and *MCEMP1* in ox-LDL-treated HUVECs

In ox-LDL-treated HUVECs, the HUVECs were exposed to ox-LDL (50 and 100 µg/mL) for 24 h. The impact on cell viability was assessed using a CCK-8 assay, which indicated that the cultured HUVECs displayed reduced cell viability after both 50 and 100 µg/mL ox-LDL treatment (Fig. 4A). Additionally, ox-LDL induced cellular injury in HUVECs, as evidenced by remarkably increased LDH and decreased NO in all tested concentrations (Figs. 4B and 4C). Moreover, the expression of ICAM1 was upregulated in response to both concentrations of ox-LDL (Fig. 4D).

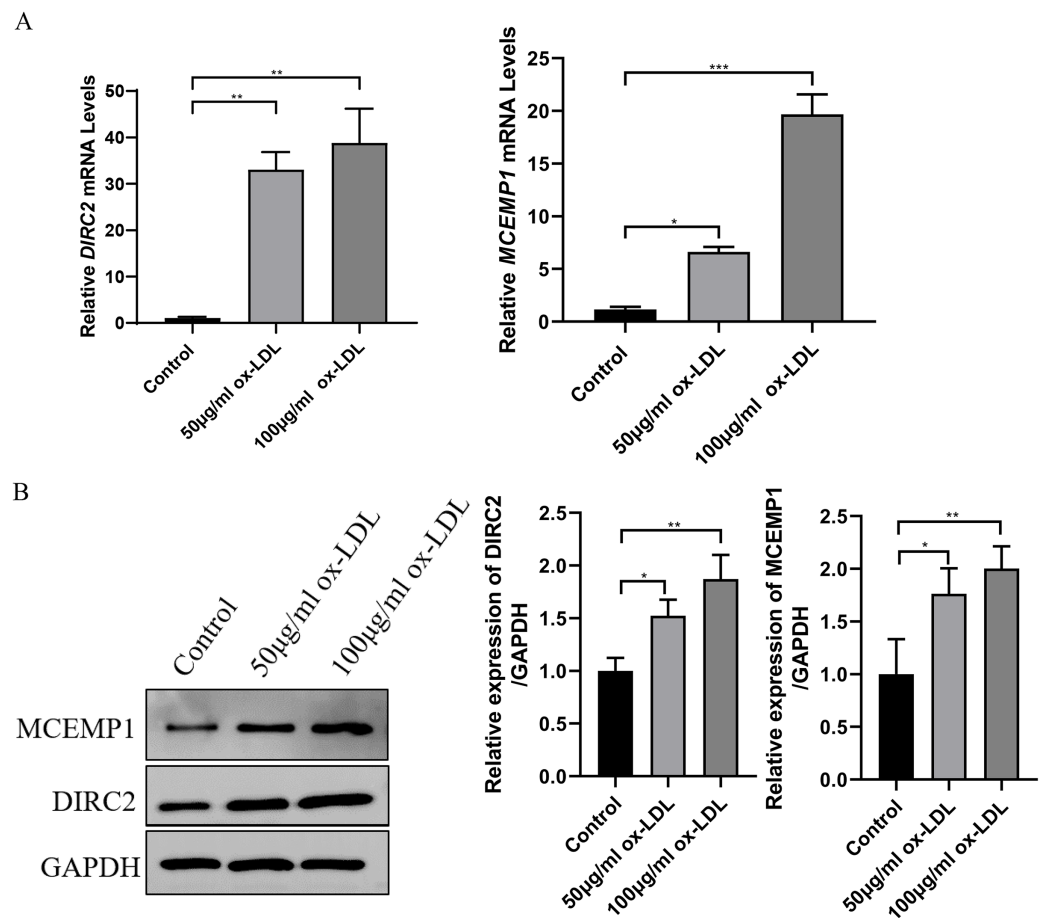


**Figure 5** The expression of *DIRC2* and *MCEMP1* in ox-LDL-treated HUVECs. (A) The mRNA and protein expression of *DIRC2* and *MCEMP1* in ox-LDL-treated HUVECs by qRT-PCR assay and Western blot assay. \* $p < 0.05$ ; \*\* $p < 0.01$ ; \*\*\* $p < 0.001$ . ox-LDL, oxidized low-density lipoprotein; HUVECs, human umbilical vein endothelial cells; qRT-PCR, quantitative real-time polymerase chain reaction.

Full-size DOI: [10.7717/peerj.18135/fig-5](https://doi.org/10.7717/peerj.18135/fig-5)

Western blot assay and qRT-PCR revealed that both the mRNA and protein levels of *DIRC2* and *MCEMP1* were upregulated in ox-LDL-treated HUVECs (Fig. 5), which was consistent with the results obtained from bioinformatics analysis. Based on these results, the *MCEMP1* gene with a high expression level was selected for subsequent experiments.

### Low expression of *MCEMP1* promoted the dysfunction of ox-LDL-treated HUVECs

To explore the role of *MCEMP1* in the dysfunction of ox-LDL-treated HUVECs, interference sequences targeting *MCEMP1* were synthesized. The interference efficiency was evaluated in HUVECs, as shown in Fig. S2. Both si*MCEMP1*-1 and si*MCEMP1*-2 were selected for subsequent experiments. Interference sequences for *MCEMP1* significantly reduced the ox-LDL-induced expression of *MCEMP1*, especially si*MCEMP1*-1 and si*MCEMP1*-2 (both  $p < 0.001$ , Figs. 6A and 6B).

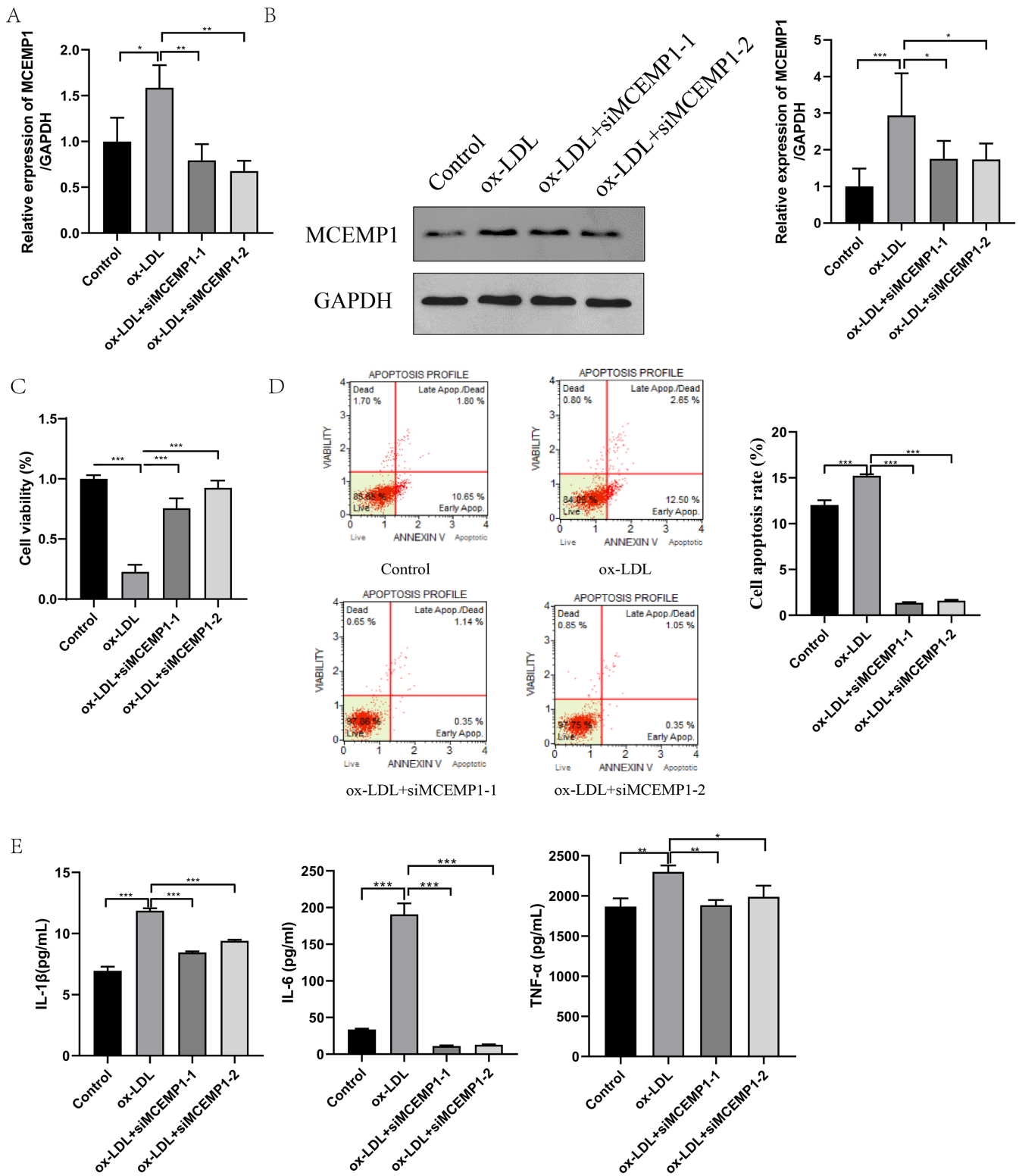


**Figure 6** Low expression of *MCEMP1* promoted the dysfunction of ox-LDL-treated HUVECs. The expression of *MCEMP1* in ox-LDL-treated HUVECs by qRT-PCR (A) and Western blot (B). The effect of *MCEMP1* knockdown on cell viability by CCK-8 assay. (C) The effect of *MCEMP1* knockdown on cell apoptosis by Muse<sup>®</sup> Cell Analyzer. (D) The levels of IL-1 $\beta$ , IL-6, and TNF- $\alpha$  in ox-LDL-treated HUVECs by ELISA Kits. \* $p < 0.05$ ; \*\* $p < 0.01$ ; \*\*\* $p < 0.001$ . ox-LDL, oxidized low-density lipoprotein; HUVECs, human umbilical vein endothelial cells; qRT-PCR, quantitative real-time polymerase chain reaction; ELISA, enzyme-linked immunosorbent assay. [Full-size !\[\]\(5f471a71b78d7676bc356df190b88ab4\_img.jpg\) DOI: 10.7717/peerj.18135/fig-6](https://doi.org/10.7717/peerj.18135/fig-6)

The effect of *MCEMP1* knockdown on the function of ox-LDL-treated HUVECs was investigated. The results, shown in Figs. 6C–6E, indicated that *MCEMP1* knockdown promoted cell proliferation ( $p < 0.01$ , Fig. 6C) but inhibited apoptosis ( $p < 0.001$ , Fig. 6D). Additionally, *MCEMP1* knockdown appeared to decrease the expression of inflammatory cytokines IL-1 $\beta$ , IL-6, and TNF- $\alpha$  (Fig. 6E). Collectively, these findings suggested that *MCEMP1* knockdown could inhibit the inflammation response in ox-LDL-treated HUVECs.

## DISCUSSION

This study aimed to uncover the key characteristic genes associated with CAD by integrating from three CAD datasets. Utilizing bioinformatics analyses and machine learning algorithms, two upregulated genes (*DIRC2* and *MCEMP1*) were identified in both the metadata and validation databases. GSEA analysis indicated a significant association of *DIRC2* and *MCEMP1* genes with infection and inflammation pathways. Furthermore, the CIBERSORT algorithm revealed a correlation between these genes and immune cell infiltration, suggesting a role in the immune response in CAD. Moreover, mRNA and protein levels of *DIRC2* and *MCEMP1* were upregulated in ox-LDL-treated HUVECs, aligning with the bioinformatics findings. Importantly, *MCEMP1* knockdown accelerated cell proliferation and suppressed cell apoptosis for ox-LDL-treated HUVECs. Additionally, *MCEMP1* knockdown might also reduce the expression of inflammatory factors IL-1 $\beta$ , IL-6, and TNF- $\alpha$ , further implicating this gene in the inflammatory processes associated with CAD.

The GEO database serves as a vital international public repository, facilitating the archiving and freely downloading high-throughput gene expression and other functional genomics datasets (Clough & Barrett, 2016). In our study, four down-regulated genes and 69 up-regulated genes were identified between CAD and control samples in a metadata cohort by merging two GEO datasets. GO analysis suggested that these DEGs might be involved in processes such as platelet aggregation regulation, defense response or response to the bacterium, regulation of amyloid precursor protein catabolic process, and positive regulation of cytokine production. These findings are consistent with previously identified CAD-related factors. Platelets are key regulators of thrombosis and inflammation and play an important role in the formation of atherothrombosis (Gawaz, Langer & May, 2005). Previous studies have reported the link between gut bacteria and atherosclerosis (Yoshida et al., 2018). One study found that amyloid protein was associated with atherosclerotic cardiovascular disease (Bampatsias et al., 2022). Cytokines are key regulators of the immune response and are involved in coronary atherosclerotic plaque and thrombosis (Yang et al., 2020). A subsequent enrichment analysis found that these DEGs were primarily related to lipid and atherosclerosis, the NF-kappa B signaling pathway, the B cell receptor signaling pathway, the IL-17 signaling pathway, the toll-like receptor signaling pathway, and the TNF signaling pathway. The NF- $\kappa$ B/ TNF signaling pathway is involved in the pathogenesis of CAD by inducing inflammation (Guo et al., 2018; Qiu et al., 2016). The IL-17/IL-10 signaling pathway is associated with the complexity of coronary atherosclerosis (Li et al., 2021). The activation of toll-like receptor signaling is involved in

chronic inflammation in CAD (Rotter et al., 2019). These signaling pathways play a role in the inflammatory response, thus influencing the occurrence and development of CAD. These results suggest that DEG is enriched in inflammation and atherosclerosis in CAD.

Machine learning algorithms are powerful tools for predicting disease from large and complex datasets employing various statistical, probabilistic, and optimization methods (Uddin et al., 2019). LASSO is the only property of the absolute value of the penalized regression coefficient. The greater the penalty, the greater the shrinkage of the coefficient, and then remove the unimportant covariates. The SVM-RFE algorithm is a sequential backward selection algorithm based on the maximum interval principle of SVM (Huang et al., 2018). Its purpose is to classify data points by maximizing the margin between classes in high-dimensional space. Both algorithm can compress coefficients of variables by constructing penalty functions and by making some regression coefficients become zero, thus achieving the purpose of variable selection (Omranian et al., 2016). Through cross-validation, the SVM-REF and LASSO algorithms reduce the risk of overfitting. In this study, these two machine-learning algorithms were used to select hub genes among 73 DEGs in a metadata cohort. Seven overlapping candidate genes (*HSDL2*, *PGLYRP1*, *CAMP*, *MCEMP1*, *IRAK3*, *DIRC2*, and *PFKFB3*) identified by both algorithms were selected for further analysis. The expression patterns of these seven hub genes in a validation data set confirmed the consistency of *DIRC2* and *MCEMP1* with the metadata set, leading to their selection for subsequent analysis.

*DIRC2* (disrupted in renal cancer 2), also named *SLC49A4*, encodes an evolutionary conserved transmembrane protein and is a novel member of the major facilitator superfamily of transporters (Bodmer et al., 2002). Functioning as an electrogenic lysosomal metabolite transporter, overexpression of *DIRC2* leads to decreased pyridoxine accumulation in cells and is associated with decreased lysosome accumulation (Akino et al., 2023). This protein may be involved in responses to extracellular signals by mediating critical protein-protein interactions (Bodmer et al., 2002). However, few studies have clarified the relationship of this gene to CAD. *MCEMP1* (mast cell-expressed membrane protein 1) gene, alternatively named *C19OFR59*, located on human chromosome 19p13.3, is a transmembrane protein expressed in mast cells, macrophages, and even the brain tissue (Strbian et al., 2006). It has been suggested that downregulation of *MCEMP1* led to a decrease in interleukin and interferon, promoting apoptosis of inflammation-inhibiting cells in sepsis (Xie et al., 2020). *MCEMP1* may also participate in regulating mast cell differentiation, the immune response, and the inflammatory response (Christie & Henderson, 2002). *MCEMP1* loss can promote the activity of T lymphocytes and NK cells, increase the expression of immunoglobulin, inhibit the release of inflammatory factors, and reduce the apoptosis of T lymphocytes (Zhou et al., 2022). *MCEMP1* has also been identified as a potential biomarker for stroke prognosis (Raman et al., 2016). Machine learning algorithms have also identified *MCEMP1* as a crucial gene in aortic dissection and cardioembolic stroke (Zhang et al., 2022; Li et al., 2022). In our study, both mRNA and protein levels of *DIRC2* and *MCEMP1* were upregulated in ox-LDL-treated HUVECs, which was consistent with bioinformatics analysis. These results

indicated that *DIRC2* and *MCEMP1* might play significant roles in the pathophysiology of CAD. Notably, *MCEMP1* knockdown promoted cell proliferation, but inhibited apoptosis in ox-LDL-treated HUVECs. Moreover, *MCEMP1* could inhibit the inflammation response in ox-LDL-treated HUVECs.

Atherosclerosis, the major cause of CAD, is characterized by hyperlipidemia and inflammation (*Weber & Noels, 2011*). In this study, the CIBERSORT program was utilized to assess immune cell infiltration profiles in CAD subjects and in healthy controls. The proportions of resting dendritic cells, resting mast cells, and regulatory T cells were decreased in CAD tissues compared to normal tissues. Conversely, there was increased infiltration of activated mast cells and neutrophils in CAD tissues. Dendritic cells are found in atherosclerotic lesions that cause inflammation of blood vessels (*Yilmaz et al., 2009*). Homeostatic Treg defect has been reported to be related to subclinical proinflammatory and atherogenic states (*Hasib et al., 2016*). Neutrophils are important components involved in immune inflammation, and elevated levels of neutrophil myeloperoxidase may lead to coronary atherosclerosis (*Wang et al., 2016*). These studies support the influence of inflammatory cells on the pathogenesis of CAD, aligning with the results of our study. *DIRC2* was negatively correlated with regulatory T cells, CD8 T cells, resting dendritic cells, and CD4 memory activated T cells but positively correlated with activated NK cells and neutrophils. *MCEMP1* was negatively associated with regulatory T cells, resting dendritic cells, and CD4 memory activated T cells, but positively related to macrophages M0, CD4 naive T cells, monocytes, activated mast cells, and neutrophils. These results indicate that the main mechanism of *DIRC2* and *MCEMP1* in CAD may be related to immune cells. However, this hypothesis needs to be tested in subsequent experiments.

There are some limitations to this study. First, due to the absence of clinical and prognostic information, the predictive value of the identified hub genes for prognosis in CAD patients was not tested. Second, this study primarily focuses on bioinformatics analysis for the correlation of *DIRC2* and *MCEMP1* with immune cell infiltration and signaling pathways, and the function of hub genes requires *in vivo* experimental investigation. Therefore, the findings of this study need to be validated with functional trials and studies with larger clinical sample sizes. Third, the *in vitro* experiments were only carried out in HUVECs cells; therefore, further experiments should be validated in additional cell lines. Moreover, the role of *MCEMP1* in other endothelial cell functions such as migration, invasion, or angiogenesis, should be more fully understood in future studies. Fourth, the underlying mechanism by which *MCEMP1* affects inflammation remains unclear. Therefore, this study will explore the mechanism on the inflammatory response by which *MCEMP1* affects the expression level of inflammatory factors and its downstream signaling molecules in subsequent studies.

## CONCLUSION

In this study, a comprehensive bioinformatics approach was employed to identify 73 DEGs, and seven hub genes were obtained from the metadata using the SVM-RFE and

LASSO algorithms. The expressions of *DIRC2* and *MCEMP1* were validated in the validation dataset and in ox-LDL-treated HUVECs. *MCEMP1* knockdown accelerated cell proliferation and suppressed cell apoptosis for ox-LDL-treated HUVECs. *MCEMP1* knockdown could also inhibit the inflammation response in ox-LDL-treated HUVECs. These findings suggest that *MCEMP1* serves an important role in the progression of CAD. However, the clinical relevance of *MCEMP1* in larger patient cohorts and the role of *MCEMP1* in other endothelial cell functions and inflammatory response need further experimental investigation.

## ACKNOWLEDGEMENTS

The authors want to thank the participants in the study.

## ADDITIONAL INFORMATION AND DECLARATIONS

### Funding

The authors received no funding for this work.

### Competing Interests

The authors declare that they have no competing interests.

### Author Contributions

- Wei Ye conceived and designed the experiments, prepared figures and/or tables, and approved the final draft.
- Bo Shen conceived and designed the experiments, authored or reviewed drafts of the article, and approved the final draft.
- Qizhu Tang conceived and designed the experiments, prepared figures and/or tables, authored or reviewed drafts of the article, and approved the final draft.
- Chengzhi Fang analyzed the data, authored or reviewed drafts of the article, and approved the final draft.
- Lei Wang analyzed the data, authored or reviewed drafts of the article, and approved the final draft.
- Lili Xie performed the experiments, analyzed the data, prepared figures and/or tables, and approved the final draft.
- Qi He performed the experiments, prepared figures and/or tables, and approved the final draft.

### Data Availability

The following information was supplied regarding data availability:

The raw measurements are available in the [Supplemental Files](#).

The flow cytometry data is available at Zenodo: Bo, S. (2024). Identification of A Novel Immune Infiltration-related Gene Signature *MCEMP1* for coronary artery disease. Zenodo. <https://doi.org/10.5281/zenodo.11171072>.



## Supplemental Information

Supplemental information for this article can be found online at <http://dx.doi.org/10.7717/peerj.18135#supplemental-information>.

## REFERENCES

- Akino S, Yasujima T, Yamashiro T, Yuasa H. 2023.** Disrupted in renal carcinoma 2 (DIRC2/SLC49A4) is an H(+)-driven lysosomal pyridoxine exporter. *Life Science Alliance* **6(2)**:e202201629 DOI [10.26508/lsa.202201629](https://doi.org/10.26508/lsa.202201629).
- Balashanmugam MV, Shivanandappa TB, Nagarethinam S, Vastrad B, Vastrad C. 2019.** Analysis of differentially expressed genes in coronary artery disease by integrated microarray analysis. *Biomolecules* **10(1)**:35 DOI [10.3390/biom10010035](https://doi.org/10.3390/biom10010035).
- Bampatsias D, Mavroeidis I, Tual-Chalot S, Vlachogiannis NI, Bonini F, Sachse M, Mavraganis G, Maretì A, Kritsioti C, Laina A, Delialis D, Ciliberti G, Sopova K, Gatsiou A, Martelli F, Georgiopoulou G, Stellos K, Stamatielopoulou K. 2022.** Beta-secretase-1 antisense RNA is associated with vascular ageing and atherosclerotic cardiovascular disease. *Thrombosis and Haemostasis* **122(11)**:1932–1942 DOI [10.1055/a-1914-2094](https://doi.org/10.1055/a-1914-2094).
- Barrett T, Wilhite SE, Ledoux P, Evangelista C, Kim IF, Tomashevsky M, Marshall KA, Phillippy KH, Sherman PM, Holko M, Yefanov A, Lee H, Zhang N, Robertson CL, Serova N, Davis S, Soboleva A. 2013.** NCBI GEO: archive for functional genomics data sets–update. *Nucleic Acids Research* **41(Database issue)**:D991–D995 DOI [10.1093/nar/gks1193](https://doi.org/10.1093/nar/gks1193).
- Behzadi P, Ranjbar R. 2019.** DNA microarray technology and bioinformatic web services. *Acta Microbiologica et Immunologica Hungarica* **66(1)**:19–30 DOI [10.1556/030.65.2018.028](https://doi.org/10.1556/030.65.2018.028).
- Bodmer D, Eleveld M, Kater-Baats E, Janssen I, Janssen B, Weterman M, Schoenmakers E, Nickerson M, Linehan M, Zbar B, van Kessel AG. 2002.** Disruption of a novel MFS transporter gene, DIRC2, by a familial renal cell carcinoma-associated t(2;3)(q35;q21). *Human Molecular Genetics* **11(6)**:641–649 DOI [10.1093/hmg/11.6.641](https://doi.org/10.1093/hmg/11.6.641).
- Bodmer D, Janssen I, Jonkers Y, van den Berg E, Dijkhuizen T, Debiec-Rychter M, Schoenmakers E, van Kessel AG. 2002.** Molecular cytogenetic analysis of clustered sporadic and familial renal cell carcinoma-associated 3q13 approximately q22 breakpoints. *Cancer Genetics and Cytogenetics* **136(2)**:95–100 DOI [10.1016/S0165-4608\(02\)00517-4](https://doi.org/10.1016/S0165-4608(02)00517-4).
- Chen JX, He S, Wang YJ, Gan XK, Zhou YQ, Hua L, Hou C, Zhang S, Zhou HX, Jia EZ. 2021.** Comprehensive analysis of mRNA expression profiling and identification of potential diagnostic biomarkers in coronary artery disease. *ACS Omega* **6(37)**:24016–24026 DOI [10.1021/acsomega.1c03171](https://doi.org/10.1021/acsomega.1c03171).
- Christie PE, Henderson WR Jr. 2002.** Lipid inflammatory mediators: leukotrienes, prostaglandins, platelet-activating factor. *Clinical Allergy and Immunology* **16**:233–254.
- Clough E, Barrett T. 2016.** The gene expression omnibus database. *Methods in Molecular Biology* **1418**:93–110 DOI [10.1007/978-1-4939-3578-9](https://doi.org/10.1007/978-1-4939-3578-9).
- Di M, Zhang Y, Zeng R, Liu X, Chen W, Zhang M, Zhang C, Li M, Zhang M. 2021.** The pro-angiogenesis effect of miR33a-5p/Ets-1/DKK1 signaling in ox-LDL induced HUVECs. *International Journal of Biological Sciences* **17(15)**:4122–4139 DOI [10.7150/ijbs.60302](https://doi.org/10.7150/ijbs.60302).
- Donovan MJ, Fernandez G, Scott R, Khan FM, Zeineh J, Koll G, Gladoun N, Charytonowicz E, Tewari A, Cordon-Cardo C. 2018.** Development and validation of a novel automated Gleason grade and molecular profile that define a highly predictive prostate cancer progression algorithm-based test. *Prostate Cancer and Prostatic Diseases* **21(4)**:594–603 DOI [10.1038/s41391-018-0067-4](https://doi.org/10.1038/s41391-018-0067-4).

- Ehret GB, Ferreira T, Chasman DI, Jackson AU, Schmidt EM, Johnson T, Thorleifsson G, Luan J, Donnelly LA, Kanoni S, Petersen AK, Pihur V, Strawbridge RJ, Shungin D, Hughes MF, Meirelles O, Kaakinen M, Bouatia-Naji N, Kristiansson K, Shah S, Kleber ME, Guo X, Lyytikäinen LP, Fava C, Eriksson N, Nolte IM, Magnusson PK, Salfati EL, Rallidis LS, Theusch E, Smith AJP, Folkersen L, Witkowska K, Pers TH, Joehanes R, Kim SK, Lataniotis L, Jansen R, Johnson AD, Warren H, Kim YJ, Zhao W, Wu Y, Tayo BO, Bochud M, CHARGE-EchoGen consortium, CHARGE-HF consortium, Wellcome Trust Case Control Consortium, Absher D, Adair LS, Amin N, Arking DE, Axelsson T, Baldassarre D, Balkau B, Bandinelli S, Barnes MR, Barroso I, Bevan S, Bis JC, Bjornsdottir G, Boehnke M, Boerwinkle E, Bonnycastle LL, Boomsma DI, Bornstein SR, Brown MJ, Burnier M, Cabrera CP, Chambers JC, Chang IS, Cheng CY, Chines PS, Chung RH, Collins FS, Connell JM, Döring A, Dallongeville J, Danesh J, de Faire U, Delgado G, Dominiczak AF, Doney ASF, Drenos F, Edkins S, Eicher JD, Elosua R, Enroth S, Erdmann J, Eriksson P, Esko T, Evangelou E, Evans A, Fall T, Farrall M, Felix JF, Ferrières J, Ferrucci L, Fornage M, Forrester T, Franceschini N, Duran OHF, Franco-Cereceda A, Fraser RM, Ganesh SK, Gao H, Gertow K, Gianfagna F, Gigante B, Giulianini F, Goel A, Goodall AH, Goodarzi MO, Gorski M, Gräßler J, Groves C, Gudnason V, Gyllenstein U, Hallmans G, Hartikainen AL, Hassinen M, Havulinna AS, Hayward C, Herberg S, Herzig KH, Hicks AA, Hingorani AD, Hirschhorn JN, Hofman A, Holmen J, Holmen OL, Hottenga JJ, Howard P, Hsiung CA, Hunt SC, Ikram MA, Illig T, Iribarren C, Jensen RA, Kähönen M, Kang H, Kathiresan S, Keating BJ, Khaw KT, Kim YK, Kim E, Kivimaki M, Klopp N, Kolovou G, Komulainen P, Kooner JS, Kosova G, Krauss RM, Kuh D, Kutalik Z, Kuusisto J, Kvaløy K, Lakka TA, Lee NR, Lee IT, Lee WJ, Levy D, Li X, Liang KW, Lin H, Lin L, Lindström J, Lobbens S, Männistö S, Müller G, Müller-Nurasyid M, Mach F, Markus HS, Marouli E, McCarthy MI, McKenzie CA, Meneton P, Menni C, Metspalu A, Mijatovic V, Moilanen L, Montasser ME, Morris AD, Morrison AC, Mulas A, Nagaraja R, Narisu N, Nikus K, O'Donnell CJ, O'Reilly PF, Ong KK, Paccaud F, Palmer CD, Parsa A, Pedersen NL, Penninx BW, Perola M, Peters A, Poulter N, Pramstaller PP, et al. 2016. The genetics of blood pressure regulation and its target organs from association studies in 342,415 individuals. *Nature Genetics* 48(10):1171–1184 DOI 10.1038/ng.3667.
- Gawaz M, Langer H, May AE. 2005. Platelets in inflammation and atherogenesis. *The Journal of Clinical Investigation* 115(12):3378–3384 DOI 10.1172/JCI27196.
- GBD 2016 Disease and Injury Incidence and Prevalence Collaborators. 2017. Global, regional, and national incidence, prevalence, and years lived with disability for 328 diseases and injuries for 195 countries, 1990–2016: a systematic analysis for the Global Burden of Disease Study 2016. *Lancet* 390(10100):1211–1259 DOI 10.1016/S0140-6736(17)32154-2.
- Guo F, Tang C, Li Y, Liu Y, Lv P, Wang W, Mu Y. 2018. The interplay of lncRNA ANRIL and miR-181b on the inflammation-relevant coronary artery disease through mediating NF-κB signalling pathway. *Journal of Cellular and Molecular Medicine* 22(10):5062–5075 DOI 10.1111/jcmm.13790.
- Harismendy O, Notani D, Song X, Rahim NG, Tanasa B, Heintzman N, Ren B, Fu XD, Topol EJ, Rosenfeld MG, Frazer KA. 2011. 9p21 DNA variants associated with coronary artery disease impair interferon-γ signalling response. *Nature* 470(7333):264–268 DOI 10.1038/nature09753.
- Hasib L, Lundberg AK, Zachrisson H, Ernerudh J, Jonasson L. 2016. Functional and homeostatic defects of regulatory T cells in patients with coronary artery disease. *Journal of Internal Medicine* 279(1):63–77 DOI 10.1111/joim.12398.

- Huang S, Cai N, Pacheco PP, Narrandes S, Wang Y, Xu W. 2018. Applications of support vector machine (SVM) learning in cancer genomics. *Cancer Genomics & Proteomics* 15(1):41–51 DOI 10.21873/cgp.20063.
- Kalayinia S, Goodarzynejad H, Maleki M, Mahdih N. 2018. Next generation sequencing applications for cardiovascular disease. *Annals of Medicine* 50(2):91–109 DOI 10.1080/07853890.2017.1392595.
- Kang H, Yu H, Fan J, Cao G. 2021. Rotigotine protects against oxidized low-density lipoprotein (ox-LDL)-induced damages in human umbilical vein endothelial cells(HUVECs). *Bioengineered* 12(2):10568–10579 DOI 10.1080/21655979.2021.2000224.
- Kott KA, Vernon ST, Hansen T, de Dreu M, Das SK, Powell J, Fazekas de St Groth B, Di Bartolo BA, McGuire HM, Figtree GA. 2020. Single-cell immune profiling in coronary artery disease: the role of state-of-the-art immunophenotyping with mass cytometry in the diagnosis of atherosclerosis. *Journal of the American Heart Association* 9(24):e017759 DOI 10.1161/JAHA.120.017759.
- Li Q, Gao X, Luo X, Wu Q, He J, Liu Y, Xue Y, Wu S, Rao F. 2022. Identification of hub genes associated with immune infiltration in cardioembolic stroke by whole blood transcriptome analysis. *Disease Markers* 2022:8086991 DOI 10.1155/2022/8086991.
- Li Q, Liu Y, Xia X, Sun H, Gao J, Ren Q, Zhou T, Ma C, Xia J, Yin C. 2021. Activation of macrophage TBK1-HIF-1 $\alpha$ -mediated IL-17/IL-10 signaling by hyperglycemia aggravates the complexity of coronary atherosclerosis: an in vivo and in vitro study. *FASEB Journal: Official Publication of the Federation of American Societies for Experimental Biology* 35(5):e21609 DOI 10.1096/fj.202100086RR.
- Li Y, Lu S, Lan M, Peng X, Zhang Z, Lang J. 2020. A prognostic nomogram integrating novel biomarkers identified by machine learning for cervical squamous cell carcinoma. *Journal of Translational Medicine* 18(1):223 DOI 10.1186/s12967-020-02387-9.
- Ma LY, Chen WW, Gao RL, Liu LS, Zhu ML, Wang YJ, Wu ZS, Li HJ, Gu DF, Yang YJ, Zheng Z, Hu SS. 2020. China cardiovascular diseases report 2018: an updated summary. *Journal of Geriatric Cardiology* 17(1):1–8 DOI 10.11909/j.issn.1671-5411.2020.01.001.
- Malakar AK, Choudhury D, Halder B, Paul P, Uddin A, Chakraborty S. 2019. A review on coronary artery disease, its risk factors, and therapeutics. *Journal of Cellular Physiology* 234(10):16812–16823 DOI 10.1002/jcp.28350.
- Medina-Leyte DJ, Zepeda-García O, Domínguez-Pérez M, González-Garrido A, Villarreal-Molina T, Jacobo-Albavera L. 2021. Endothelial dysfunction, inflammation and coronary artery disease: potential biomarkers and promising therapeutical approaches. *International Journal of Molecular Sciences* 22(8):3850 DOI 10.3390/ijms22083850.
- Milutinović A, Šuput D, Zorc-Pleskovič R. 2020. Pathogenesis of atherosclerosis in the tunica intima, media, and adventitia of coronary arteries: an updated review. *Bosnian Journal of Basic Medical Sciences* 20(1):21–30 DOI 10.17305/bjbms.2019.4320.
- Newman JL, Stone JR. 2019. Immune checkpoint inhibition alters the inflammatory cell composition of human coronary artery atherosclerosis. *Cardiovascular Pathology* 43:107148 DOI 10.1016/j.carpath.2019.107148.
- Omranian N, Eloundou-Mbebi JM, Mueller-Roeber B, Nikoloski Z. 2016. Gene regulatory network inference using fused LASSO on multiple data sets. *Scientific Reports* 6:20533 DOI 10.1038/srep20533.

- Qi B, Chen JH, Tao L, Zhu CM, Wang Y, Deng GX, Miao L. 2020. Integrated weighted gene co-expression network analysis identified that TLR2 and CD40 are related to coronary artery disease. *Frontiers in Genetics* 11:613744 DOI 10.3389/fgene.2020.613744.
- Qiu HN, Liu B, Liu W, Liu S. 2016. Interleukin-27 enhances TNF- $\alpha$ -mediated activation of human coronary artery endothelial cells. *Molecular and Cellular Biochemistry* 411(1–2):1–10 DOI 10.1007/s11010-015-2563-3.
- Raman K, O'Donnell MJ, Czlonkowska A, Duarte YC, Lopez-Jaramillo P, Peñaherrera E, Sharma M, Shoamanesh A, Skowronska M, Yusuf S, Paré G. 2016. Peripheral blood MCEMP1 gene expression as a biomarker for stroke prognosis. *Stroke* 47(3):652–658 DOI 10.1161/STROKEAHA.115.011854.
- Rotter SV, Sandstedt J, Johansson M, Lundqvist A, Bergström G, Jeppsson A, Mattsson HL. 2019. Toll-like receptor-mediated inflammation markers are strongly induced in heart tissue in patients with cardiac disease under both ischemic and non-ischemic conditions. *International Journal of Cardiology* 293:238–247 DOI 10.1016/j.ijcard.2019.06.033.
- Strbian D, Karjalainen-Lindsberg ML, Tatlisumak T, Lindsberg PJ. 2006. Cerebral mast cells regulate early ischemic brain swelling and neutrophil accumulation. *Journal of Cerebral Blood Flow and Metabolism* 26(5):605–612 DOI 10.1038/sj.jcbfm.9600228.
- Uddin S, Khan A, Hossain ME, Moni MA. 2019. Comparing different supervised machine learning algorithms for disease prediction. *BMC Medical Informatics and Decision Making* 19:281 DOI 10.1186/s12911-019-1004-8.
- Wang XS, Kim HB, Szuchman-Sapir A, McMahon A, Dennis JM, Witting PK. 2016. Neutrophils recruited to the myocardium after acute experimental myocardial infarct generate hypochlorous acid that oxidizes cardiac myoglobin. *Archives of Biochemistry and Biophysics* 612:103–114 DOI 10.1016/j.abb.2016.10.013.
- Wang C, Song C, Liu Q, Zhang R, Fu R, Wang H, Yin D, Song W, Zhang H, Dou K. 2021. Gene expression analysis suggests immunological changes of peripheral blood monocytes in the progression of patients with coronary artery disease. *Frontiers in Genetics* 12:641117 DOI 10.3389/fgene.2021.641117.
- Weber C, Noels H. 2011. Atherosclerosis: current pathogenesis and therapeutic options. *Nature Medicine* 17(11):1410–1422 DOI 10.1038/nm.2538.
- Xie W, Chen L, Chen L, Kou Q. 2020. Silencing of long non-coding RNA MALAT1 suppresses inflammation in septic mice: role of microRNA-23a in the down-regulation of MCEMP1 expression. *Inflammation Research* 69(2):179–190 DOI 10.1007/s00011-019-01306-z.
- Yang P, Liu J, Xiao J, Jian H, Chen H. 2020. Associations between seven common cytokine gene polymorphisms and coronary artery disease: evidence from a meta-analysis. *International Archives of Allergy and Immunology* 181(4):301–310 DOI 10.1159/000504752.
- Yilmaz A, Schaller T, Cicha I, Altendorf R, Stumpf C, Klinghammer L, Ludwig J, Daniel WG, Garlich CD. 2009. Predictive value of the decrease in circulating dendritic cell precursors in stable coronary artery disease. *Clinical Science* 116(4):353–363 DOI 10.1042/CS20080392.
- Yoshida N, Emoto T, Yamashita T, Watanabe H, Hayashi T, Tabata T, Hoshi N, Hatano N, Ozawa G, Sasaki N, Mizoguchi T, Amin HZ, Hirota Y, Ogawa W, Yamada T, Hirata KI. 2018. *Bacteroides vulgatus* and *bacteroides dorei* reduce gut microbial lipopolysaccharide production and inhibit atherosclerosis. *Circulation* 138(22):2486–2498 DOI 10.1161/CIRCULATIONAHA.118.033714.

**Zhang H, Chen T, Zhang Y, Lin J, Zhao W, Shi Y, Lau H, Zhang Y, Yang M, Xu C, Tang L, Xu B, Jiang J, Chen X. 2022.** Crucial genes in aortic dissection identified by weighted gene coexpression network analysis. *Journal of Immunology Research* **2022**(5):7585149  
[DOI 10.1155/2022/7585149](https://doi.org/10.1155/2022/7585149).

**Zhao M, Jin X, Chen Z, Zhang H, Zhan C, Wang H, Wang Q. 2022.** Weighted correlation network analysis of cancer stem cell-related prognostic biomarkers in esophageal squamous cell carcinoma. *Technology in Cancer Research & Treatment* **21**(5):15330338221117003  
[DOI 10.1177/15330338221117003](https://doi.org/10.1177/15330338221117003).

**Zhou J, Dong S, Wang P, Su X, Cheng L. 2022.** Identification of nine mRNA signatures for sepsis using random forest. *Computational and Mathematical Methods in Medicine* **2022**:5650024  
[DOI 10.1155/2022/5650024](https://doi.org/10.1155/2022/5650024).